A R C H I V E S O F M E T A L L U R G Y A N D M A T E R I A L S
Volume 60 2015 Issue 1
DOI: 10.1515/amm-2015-0020

M. KOPERNIK*

FAILURE STRAIN AND STRAIN-STRESS ANALYSIS IN TITANIUM NITRIDE COATINGS DEPOSITED ON RELIGA HEART EXT VENTRICULAR ASSIST DEVICE

ODKSZTAŁCENIE USZKODZENIA I ANALIZA ODKSZTAŁCENIOWO-NAPRĘŻENIOWA W POWŁOKACH AZOTKU TYTANU NANOSZONYCH NA KOMORĘ WSPOMAGANIA PRACY SERCA RELIGA HEART EXT

The Polish ventricular assist device is made of Bionate II with deposited TiN biocompatible nano-coating. The two scale finite element model is composed of a macro-model of blood chamber and a micro-model of the TiN/Bionate II. The numerical analysis of stress and strain states confirmed the possibility of fracture. Therefore, the identification of a fracture parameter considered as a failure strain is the purpose of the present work. The tensile test in a micro chamber of the SEM was performed to calibrate the fracture parameter of the material system TiN/Bionate II. The failure strain is a function of a temperature, a thickness of coating and parameters of surface's profile. The failure strain was calculated at the stage of the test, in which the initiation of fracture occurred. The finite element micro-model includes the surface roughness and the failure strain under tension condition for two thicknesses of coatings which will be deposited on the medical device.

Keywords: titanium nitride (TiN), left ventricular assist device (LVAD), finite element method (FEM), scanning electron microscopy (SEM), micro-tensile test

Polska komora wspomagania pracy serca jest wykonana z Bionate II z naniesioną biokompatybilną powłoką TiN. Dwuskalowy model elementów skończonych składa się z modelu makro czaszy krwistej i z modelu mikro dla TiN/Bionate II. Numeryczna analiza stanów naprężeń i odkształceń potwierdza prawdopodobieństwo pękania. Zatem, identyfikacja parametru pękania rozpatrywanego jako odkształcenie uszkodzenia jest celem niniejszej pracy. Próba rozciągania w komorze SEM została przeprowadzona, aby skalibrować parametr pękania dla układu materiałowego TiN/Bionate II. Odkształcenie uszkodzenia jest funkcją temperatury, grubości powłoki i parametrów profilu powierzchni. Odkształcenie uszkodzenia zostało obliczone w tym etapie testu, w którym pojawiła się inicjacja pęknięcia. Mikro model elementów skończonych zawiera chropowatość powierzchni i odkształcenie uszkodzenia w warunkach rozciągania dla dwóch grubości powłok, które będą nanoszone w tym urządzeniu medycznym.

1. Introduction

The latest studies dedicated to experimental *in situ* SEM micro tensile test are introduced briefly in the present section. In work [1], the experimental micro tensile testing was conducted upon TiAl polysynthetically twinned crystals containing single domains with 0° and 90° oriented lamellae. The orientation-dependent deformability of the Ti_3Al phase plays an important role in the micro tension deformation behaviour. Small-scale delaminations due to TiAl/Ti_3Al interlamellar cracking enhance the ductility of the 0° oriented crystal. In the 90° oriented crystal, the high degree of strength effects on the scale of a few tens of micrometres and may be attributed to the reduced probability of the weakest link. In paper [2], the *in situ* fracture experiments were performed inside the transmission electron microscope on 150-300 nm thick films fabricated from titanium nitride/titanium multi-layers with titanium nitride as the notched and titanium as unnotched layers. The terminal cracks always were nucleated at the unnotched edge of the specimens and not at the notch tip. The motion of dislocations was observed towards the notch tip. It was suggested that the room temperature dislocation activities are facilitated by the residual stresses in the multi-layer specimens. The most advanced experimental work is [3], in which an experimental methodology was developed to characterise local strain heterogeneities in alloys via *in situ* scanning electron microscope.

According to the literature studies [1,2], it is observed that quantitative measurements of local strains as a function of grain orientation, morphology and neighbourhood are crucial for mechanistic understanding and validation of the crystal plasticity models. The study [3] was focused on the technical challenges associated with performing creep tests at elevated temperatures $\leqslant$700°C in a SEM. Samples of nickel-based superalloy were used as the examined material. Electron beam lithography was employed to produce a suitable surface speckle pattern of hafnium oxide to facilitate a full field displacement measurements using a commercial software package.

* AGH UNIVERSITY OF SCIENCE AND TECHNOLOGY, FACULTY OF METALS ENGINEERING AND INDUSTRIAL COMPUTER SCIENCE, AL. A. MICKIEWICZA 30, 30-059 KRAKÓW, POLAND

The minimum strain resolution due to the SEM's image distortions was determined prior to tensile testing, and image integration methods were utilized to minimize imaging artifacts. The most common literature reports presented the typical approach to experimental micro tensile test [4-6], in which the strain-stress curves and the SEM micro photographs of specimens were obtained, for example Sn-3.0Ag-0.5Cu solder joints in [4], Ti-base and Cr-base coatings in [5] and TiN-coated steel in [6].

The second group of literature studies is dedicated to numerical modelling of *in situ* SEM micro tensile/micro compression test, in which a finite element method (FEM) [7] and a discrete dislocation dynamics (DD) [8] are applied. Thus, in the paper [7] the FE modelling of the micro compression experiments using an anisotropic crystal plasticity framework provided insight regarding changes in the internal stress field and resultant activity of slip systems of Rene N5 Ni superalloy. In work [8], the discrete dislocation simulations were conducted within a two-dimensional plane-strain framework with the dislocations modelled as line singularities in an isotropic elastic medium. Physics-based constitutive rules were employed for an adequate representation of hardening. The numerical input parameters of the simulations were directly identified from a subset of experimental data reached for Cu. Concluding, the numerical and experimental approaches were coupled in all of the cited works [7,8]. The recommended numerical methods (FEM and DD) are combined in the latest works [9] and they were dedicated to problems of mechanical behaviour of crystals from micro- to nano-scales.

Summarizing, the literature research shows that experimental *in situ* SEM micro tensile test provides detailed data for fracture analysis in a micro scale. The last fact is often examined in the literature for materials of the crystal plasticity problems. The same trend is observed in the numerical research of the tests inspired by the *in situ* SEM micro tensile/micro compression tests. The FEM and DD methods are used to solve not only problems of fracture in a micro scale, but a nano scale is also considered.

Referring to the trends presented in literature, the goal of present work is to identify the fracture parameter considered as a failure strain. The tensile test in a micro chamber of the SEM was performed to calibrate the fracture parameter of the material system TiN/Bionate II. The finite element micro-model includes the surface roughness and the failure strain under tension condition for two thicknesses of coatings which will be deposited on the medical device. The thicknesses of TiN coatings and parameters of deposition process (which have influence on roughness) have already been developed in the Polish Artificial Heart Programme [10-12]. The selected thicknesses of TiN coatings (50 nm and 100 nm) have been investigated in many types of tests (mechanical, biological, chemical) and are selected to the final version of the application.

The failure strain is determined in the TiN coating on the basis of mechanical tests and is a function of a temperature, a thickness of coating and parameters of surface's profile. The failure strain was calculated at the stage of the test, in which the initiation of fracture occurred. Thus, the failure strain provides crucial information on whether or not the coating breaks in the medical device. The numerical model of the micro tension test will be developed in the FE code [13,14] dedicated to solution of problems posed in the materials [12,10] and constructions of the Polish left ventricular assist devices (Religa Heart Ext) [11] shown in Fig. 1.

Fig. 1. Physical model of the Religa Heart Ext with marked elements: 1 – an outlet connector, 2 – an outlet mechanical valve, 3 – a pneumatic blood chamber with membrane, 4 – an inlet connector, 5 – an inlet mechanical valve

2. Materials and Methods

The progress has been achieved in evaluating the toughness of hard coatings and thin films over the past decade [15,16]. The developed methodologies are based on indentation, bending and micro tensile testing. The recent development in fracture toughness measurement involves the application of macro-tension to a substrate in order to induce micro tension in a patterned thin film. According to the latest trend presented in literature [16], the author of the present paper proposes to apply the micro-tensile testing and the FE model of the test to determinate the fracture parameters for the TiN coatings [12] deposited on the Bionate II [10]. The methodology and an example of the *in situ* SEM micro tensile test applied to calibrate the fracture model in a micro scale is given in [17].

2.1. Tension test for Bionate II 55D

The tension test for Bionate II 55D (thermoplastic polycarbonate-urethane) [18] was performed at the Foundation of Cardiac Surgery Development in Zabrze. The static uniaxial tension test was carried out for 8 specimens of Bionate II 55D in two temperatures (21°C and 37°C) and stretched with velocity 10 mm/min. Dimensions of specimens were: thickness 4.685 ± 0.131 mm and width 6.68 ± 0.112 mm for four specimens in 21°C; and thickness 4.62 ± 0.089 mm and width 6.433 ± 0.184 mm for four specimens in 37°C. The specimens were prepared in an injection method and tested on the machine MTS Criterion Single equipped with a force sensor 5 kN. The registered data was developed in the MTS TestWorks^{TM}software. Tests and calculations were performed according to the standards [18]: ISO 527-2 and ASTM D 638. The experimental results of tension test for polymer are shown in Fig. 2. The material model of polymer at 21°C will be introduced into the model of micro tensile test as identified Hollomon's material model: $36.45\varepsilon^{0.72}$.

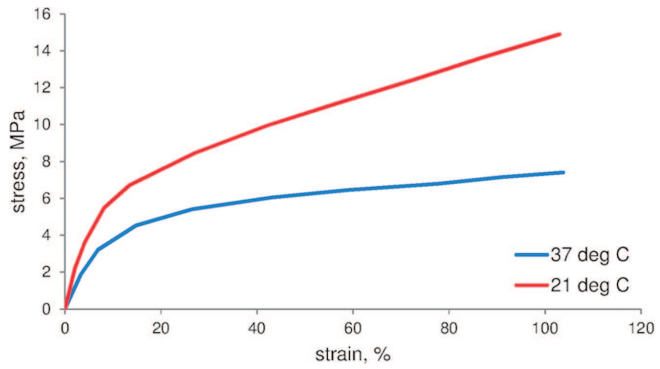

Fig. 2. Stress-strain curves of the Bionate II 55D in two temperatures (21°C and 37°C)

2.2. AFM's roughness measurement

Roughness measurements of the substrate-Bionate II and TiN coatings (50 nm, 100 nm and 500 nm) were performed at the WIMiIP AGH by using Atomic Force Microscope (AFM) (Veeco company). The roughness of a nano-coating is often approximated by a surface wave [19] defined using an antinode and a wavelength. This approach is realized in the developed numerical models [20] in a micro scale. The developed micro model was evaluated for many sets of conditions according to factor analysis what was shown in [20]. Continuing this approach, the average values of antinode and wavelength were calculated basing on the FFT of the surface profile data obtained for the TiN nano-coatings (50 nm and 100 nm) and substrate for all of the analysed areas and for all of the selected scan lines. The average wavelengths of coatings of thicknesses 50 nm and 100 nm were calculated for the area 1 μm×1 μm in several places of samples for several line scans (the examples are presented in Figs. 3-4). The bigger area of substrate of 100 μm×100 μm for several line scans were also investigated (the example is shown in Fig. 5). Thus, the developed micro model of sample represents the wave character of TiN coating, but not the wave character of the substrate. It is a local micro model.

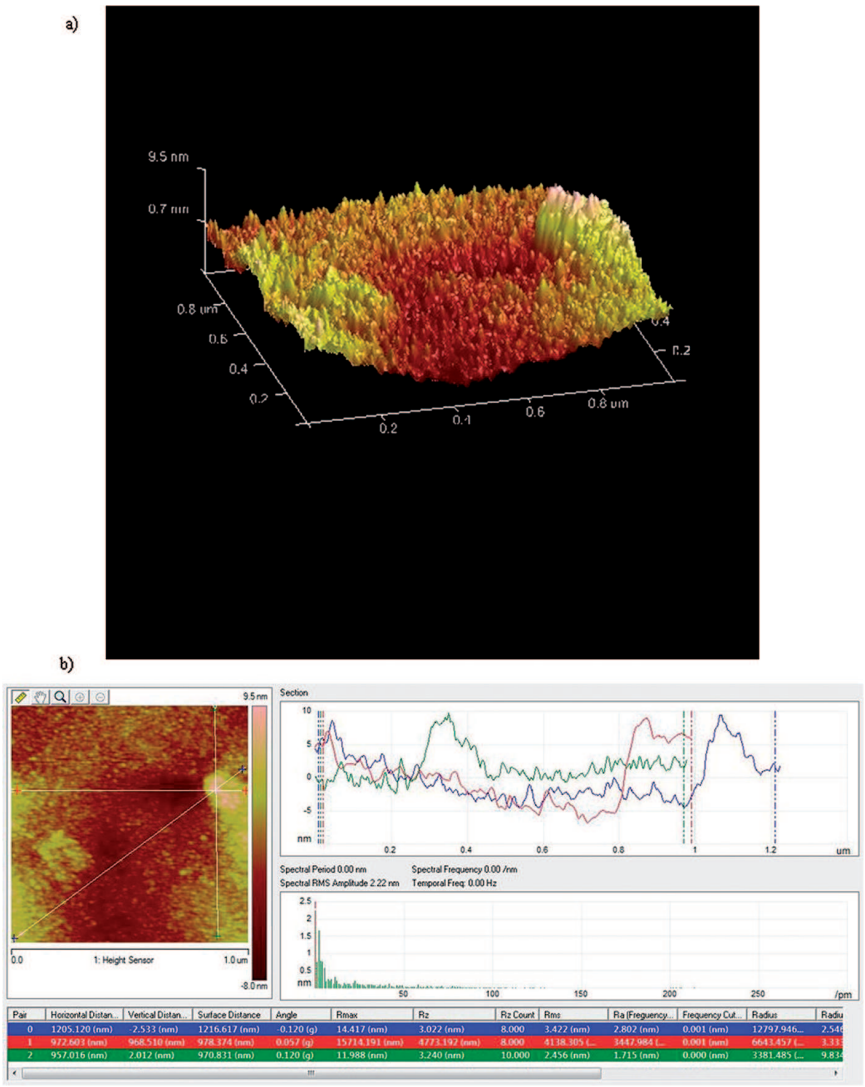

Fig. 3. The AFM's image of topography of the TiN nanocoating of thicknness 50 nm on the selected line of the area 1 μm×1 μm. b) The FFT of the surface profile corresponding to the three line scans of nanocoating of thickness 50 nm

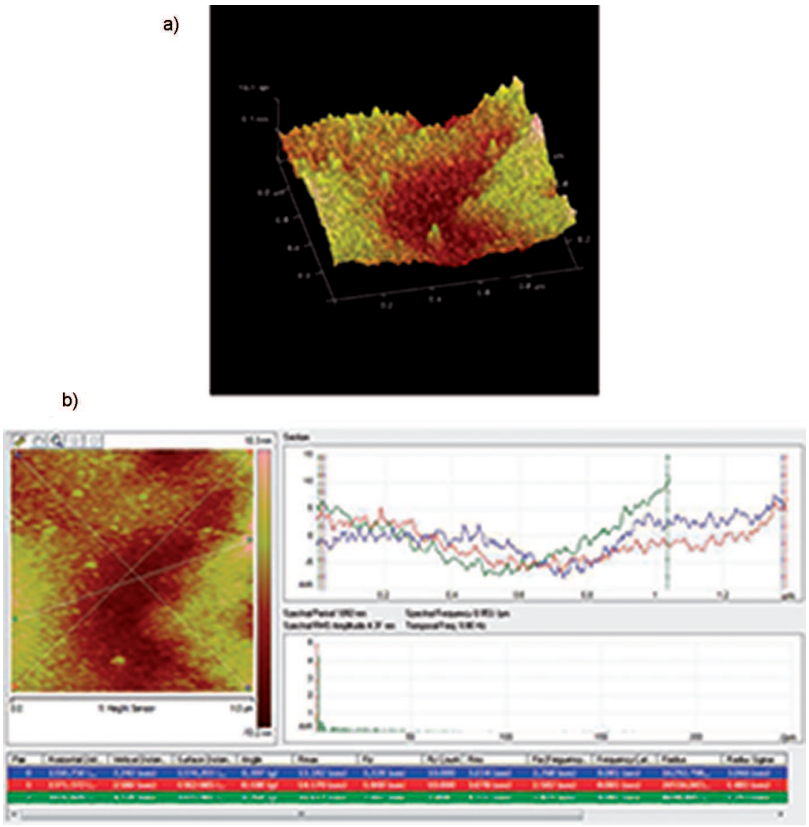

Fig. 4. a) The AFM's image of topography of the TiN nanocoating of thicknness 100 nm on the selected line of the area 1 μm×1 μm. b) The FFT of the surface profile corresponding to the three line scans of nanocoating of thickness 100 nm

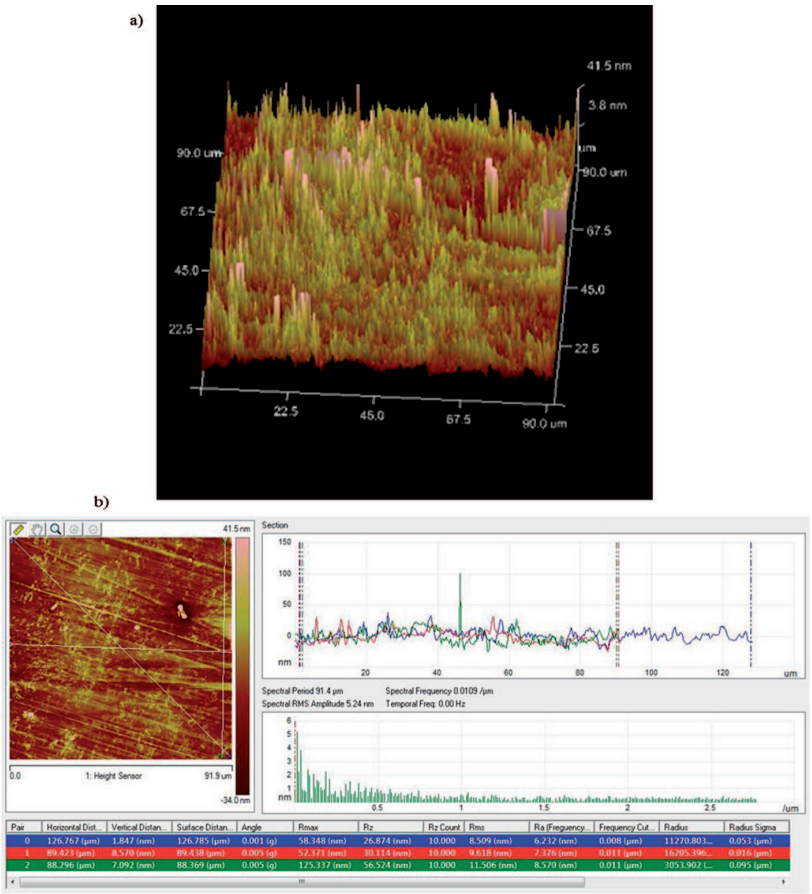

Fig. 5. The AFM's images of the substrate's topography on the selected line scan of the area 100 μm×100 μm. b) The FFT of the surface profile corresponding to the three line scans of substrate

The average calculated parameters of a sinusoidal surface of the TiN nano-coatings are: a) an antinode – 12.5 nm and a wavelength – 100 nm for TiN coating of thickness 50 nm, b) an antinode – 20 nm and a wavelength – 150 nm for TiN coating of thickness 100 nm. For polyurethane substrate R_a parameter is about 1.74 nm (for size of area *ca.* 100 nm×100 nm), 7.5 nm and 78.7 nm for sizes of areas *ca.* 1 μm×1 μm and 100 μm×100 μm.

There are many cracks in the thick TiN coatings (500 nm) after deposition process, therefore, these coatings were not studied in the micro tensile test and their wave's parameters were not calculated.

2.3. In situ SEM micro tensile test

The TiN nano-coatings of thicknesses 50 nm and 100 nm were deposited on the Bionate II substrates by using pulsed Nd:YAG laser system proposed at the WIMiIP AGH [12]. The parameters of deposition process were: 100 mJ energy of laser beam, 266 nm wavelength, 4.2 J/cm^2 fluence, 25°C temperature of substrate, 12 ns pulse duration at a repetition rate of 10 Hz, 10 000 laser impulses for the TiN coating of thickness 100 nm and 5000 laser impulses for the TiN coating of thickness 50 nm. The independent verification of thicknesses of deposited coatings was done in TEM studies. The example of TEM's result obtained for the thinner coating (50 nm) is presented in Fig. 6.

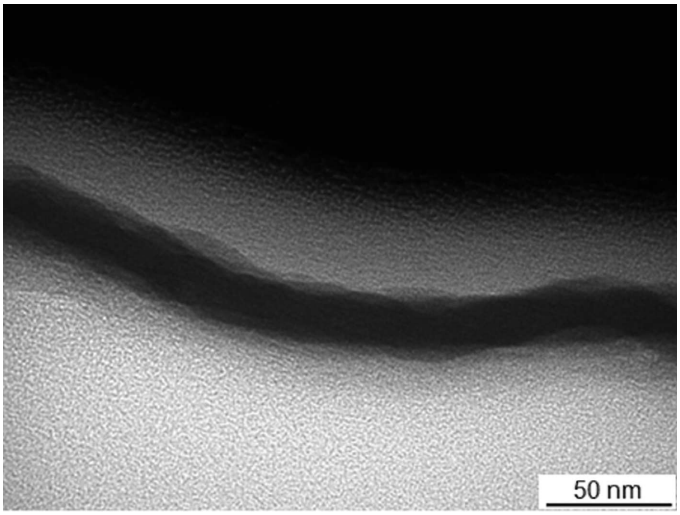

Fig. 6. The TEM's image of cross-section of the TiN coating of thickness 50 nm deposited on Bionate II

The *in situ* SEM micro tensile test was performed at the WIMiIP AGH by using Scanning Electron Microscope (SEM) Hitachi 3500 N. The specimens with the TiN coating of thickness 50 nm were stretched by a force to 40 N in 31 steps in the SEM micro chamber. The specimens with the TiN coating of thickness 100 nm were stretched by a force to 65 N in 57 steps in the SEM micro chamber. Each step of deformation for the specimens was documented by the SEM's micro photographs by using several zooms. The dimensions of the tested specimens composed of coating/substrate were: a) 50 nm of the TiN – thickness 4.15 mm, width 6.76 mm, length 32.6 mm, and b) 100 nm of the TiN – thickness 4.12 mm, width 6.2 mm, length 34.6 mm.

Because of dominant influence of soft substrate (Bionate II), it is impossible to determinate quantitatively tensile strength of the TiN layer. Thus, the most important is to achieve the failure strain for which the coating breaks in the performed experiments.

2.4. Model of micro tension test

The strain analysis on the inner surface of the Religa Heart Ext's blood chamber (acquired from the macro-scale FE model) are used to find the areas with the biggest tendency for failure. The FE elements with the maximum strain and stress are located between the two connectors [21] on the inner surface of the blood chamber. These results are further examined in the developed micro scale model. The same micro scale model enriched with boundary conditions taken from the experimental micro tensile test is used in the present work. The SEM's results represent the mean strain in direction of elongation (X) and it is the boundary condition in the micro scale model of the test (for representative volume element, RVE). The micro scale model of the TiN/polymer has surface's irregularities (roughness) due to the TiN nano-coating based on the AFM's results. The coating is represented by a periodic function [19] with three key parameters (see section 2.2): amplitude, wavelength and thickness. The micro model incorporates the experimental parameters: compressive residual stress (1 GPa), shape parameters of the coating wave's characteristics, material models of the TiN coating and the polymer (see section 2.1). The value 1 GPa is an average and typical value of residual stress given in literature for TiN coatings [22,23] deposited by physical vapour deposition methods. The author of the paper developed the value of residual stress of the TiN coating in profilometric studies and this value is close to 1 GPa [24].

The material model of TiN nano-coating was identified in [22] using results of nanoindentation test, inverse analysis and FE model. The bilinear, elastic-plastic material model of the TiN nano-coating is described by the parameters: $\varepsilon_1 = 0.009$, $\sigma_1 = 2\ 614$ MPa, $\varepsilon_2 = 0.166$ and $\sigma_2 = 9\ 107$ MPa.

The RVE is composed of the polymer and the TiN nano-coating. The non-linearity of mechanical properties of the TiN coating and the polymer are observed. Thus, an elastic-plastic and a non-linear elastic material model, as well as their corresponding theories, are used in the computations. The micro scale boundary problem, which included the unloading process, is solved by the FE micro model. The initial stress $\{\sigma_{0\,res}\}$ in the TiN nano-coating is applied in the FE formulation. The relationship between the stresses and strains is established using a matrix (vector) definition:

$$\{\sigma^m\} = [D^m]\{\varepsilon^m\} - \left\{\sigma^m_{0res}\right\} \tag{1}$$

where: $\left\{\sigma^m_{0res}\right\}$ – residual stress; $\{\sigma^m\}$ and $\{\varepsilon^m\}$ – stress and strain tensors in vector format.

The variational principle of the non-linear elastic and elastic-plastic theories led to the following functional form for the finite element e in the RVE:

$$W = \int_{V_e} \tfrac{1}{2}\{U^m\}^T[B]^T[D^m][B]\{U^m\}\,dV - \int_{V_e}\{U^m\}^T[B]^T\left\{\bar{\sigma}^m_{0res}\right\}dV - \int_{S_e}\{U^m\}^T\left[\bar{N}\right]^T\{p^m\}\,dS \tag{2}$$

where: $\{U^m\}$ – nodal displacement vector in the elements; $\bar{\sigma}^m_{0\,res}$ – experimental value of the residual stress in the current finite element e.

The effective Young's modulus is used in the elastic zone (instead of the Young's modulus) to linearise the function in Eq. (2) for a non-linear problem:

$$E^m_{eff} = \frac{\sigma^m_i}{\varepsilon^m_i}. \tag{3}$$

The stiffness matrix $[K]$ and the load vector $\{F\}$are established in the forms:

$$[K^m_e] = \int_{V_e} [B]^T [D^m] [B]\, dV \tag{4}$$

$$\{F^m_e\} = -\int_{V_e} [B]^T \left\{\bar{\sigma}^m_{0res}\right\} dV - \int_S \left[\bar{N}\right]^T \{p^m\}\, dS. \tag{5}$$

The residual stress in the TiN nano-coating is evaluated before the loading simulations. After implementation of the residual stress $\bar{\sigma}_{0\,res}$, the micro scale simulations of loading and unloading are performed.

The periodic boundary conditions (PBC) are used and the cinematic boundary conditions are applied in the direction of tension. The deformation in direction of tension ε^M_1 (first principal strain of the strain tensor) obtained in the *in situ* SEM's micro tension test as the mean X- strain is used as a boundary condition for the RVE. A strain ε^M_2 (second principal strain of the strain tensor) taken from the *in situ* SEM's micro tension test as the mean Y – strain is introduced in the micro scale model. Therefore, the 3D boundary problem of the RVE deformation is transformed to 2D plane strain problem with a prescribed value of the strain ε^M_2.

2.5. Fracture model

The methodology to extract the parameters of a facture model based on the *in situ* SEM's micro tension test was presented in [17]. The key parameter, which represents fracture is called a ductility function. Generally, this parameter is defined by the formula:

$$\psi = \frac{\varepsilon_i}{\varepsilon_p} \tag{6}$$

where: ε_i – an effective strain, ε_p – a failure stain.

The failure strain ε_p is based on the experimental tension tests at the moment of a fracture occurrence and can be a function of temperature, thickness of coating and parameters of surface's profile. Determination of the ductility function's parameters basing on the *in situ* SEM micro tension test for the two types of specimens is the goal of simulations in a micro scale.

3. Results and discussion

The main observations made in the experimental studies: AFM and SEM are briefly presented below. The AFM's data indicates that roughness of deposited coatings changes with their thickness. The roughness of the thinnest coatings (50 nm) depends strongly on the roughness of the substrate. The thinnest coatings are smooth and there are no cracks, delamination or chipping on their surfaces after deposition. The topography of the thick coatings is completely different. The thickest coatings (500 nm) have insular-columnar structure (Fig. 7). The analysis of SEM's results shows that there is an accumulation of stresses on the border areas, among islands.

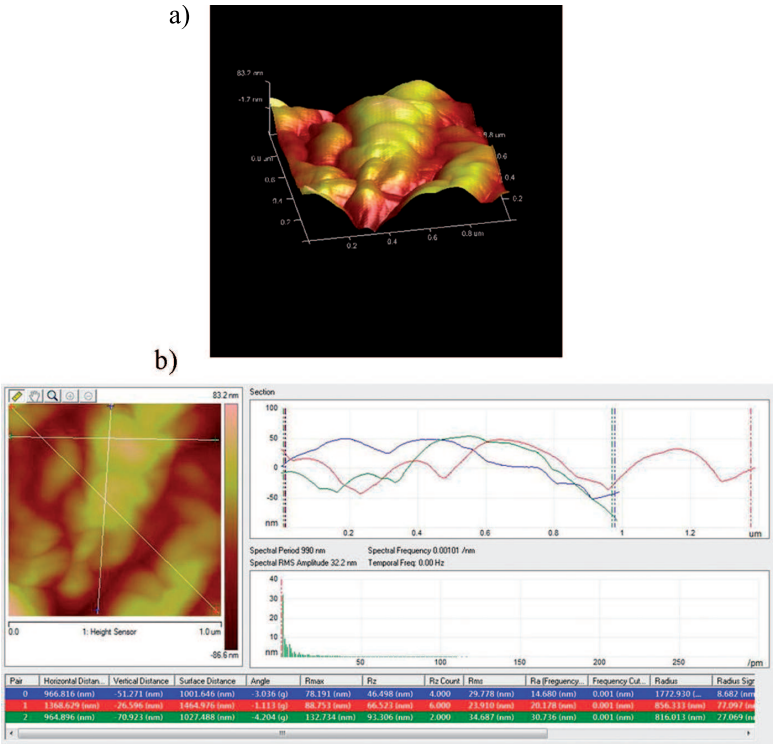

Fig. 7. a) The AFM's image of topography of the TiN nanocoating of thicknness 500 nm on the selected line of the area 1 μm×1 μm, b) The FFT of the surface profile corresponding to the three line scans of nanocoating of thickness 500 nm

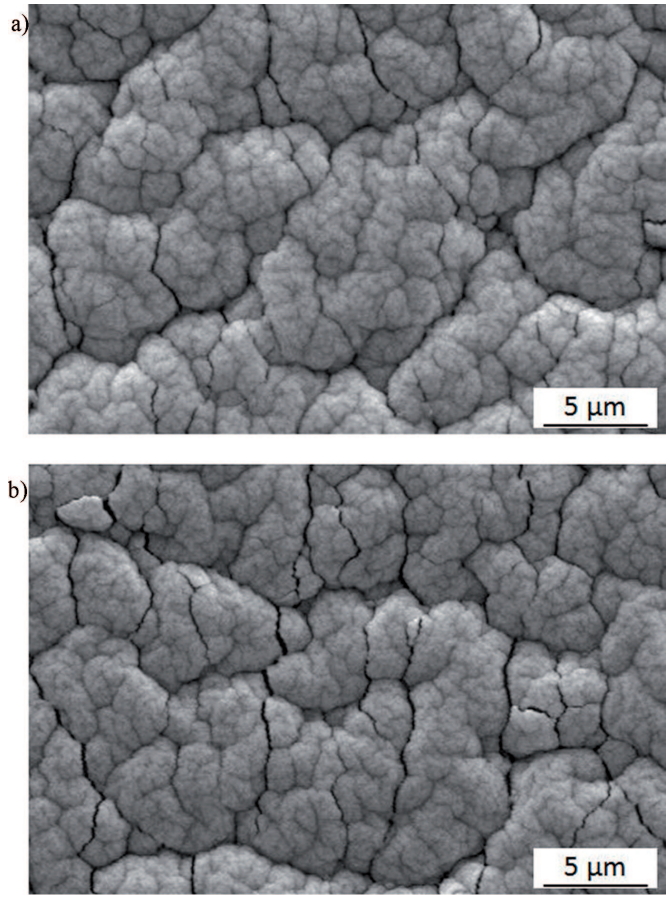

Fig. 8. The SEM's image of TiN coating of thickness 500 nm stretched at: a) 0 N and b) 15 N

Therefore, there are many cracks in these places and they are clearly visible even without external forced deformation (Fig. 8). Contrary, the thinnest coatings cracks only after external forced deformation and the cracks extend at an angle 75-85° to the stretching direction. There are some small cracks on the surface of coating at the initial stage of deformation. When the sample is stretched at about 0.2 mm, the number of cracks begins to increase rapidly. When the sample is stretched at exactly 0.2 mm, the entire sample surface is covered with cracks. It should be noted that extension of the thin TiN coating (50 nm) of about 0.2 mm causes very big deformation. The numerous cracks occur at the stretching of several μm. The cracks propagate in the perpendicular direction to the main cracks and are caused by shrink and deformation of substrate in the direction perpendicular to the stretching. The justification of cracking of the TiN coatings can be described as follows: the substrate-coating compound system always tends to reduce the overall strain energy. If the substrate material is deformable like the polymer, the huge difference in elastic moduli trigger huge deformation of the surface. Wrinkling has been suggested as a mode of common deformations of the substrate (surface) and the film in such situations (compare [25]). Wrinkling is described as the formation of sinusoidal buckles on the surface, which doesn't lose their adhesion to the substrate (which distinguishes it from buckling). Thus, the main deformation mechanisms in wrinkling are bending of the substrate or of the near-surface region of the substrate (depending of the elasticity of the substrate material) together with the covering coating (compare [24]).

Basing on settings of the experimental tensile tests, the corresponding numerical models of the tests were prepared in a micro scale. The most representative computational and experimental results of the tensile tests are shown in TABLE 1. The simulations were performed for initial, middle and final stages of the tests, which correspond to the forces 8, 15 and 40 N. There was a noticeable change in a number of cracks on the surface of specimens in the middle stages of the experimental tests, therefore these stages were used to determine the failure strain. The SEM's images taken from these stages of the tests are shown in Fig. 9a and Fig. 10a. The numerical results computed at the middle stages of the tests are presented in Figs. 9b,c and Figs. 10b,c. In the TABLE 1, the numerical results are represented by the effective strain and the mean stress. The mean value of X – strain (failure strain) was obtained in the experimental tests. The FE's effective strain is higher for the TiN coating of thickness 50 nm than for the TiN coating of thickness 100 nm at the same stages of the tests. Contrary, the FE's mean stress is higher for the TiN coating of thickness 100 nm than for the TiN coating of thickness 50 nm. This value is the same for the TiN coatings of thicknesses of 50 nm and 100 nm at the same stages of the tests. The stresses shown in TABLE 1 are high, because the residual stress is high (1 GPa) and critical loading conditions were applied (40 N). The FE's effective strain is higher than the SEM's mean X – strain at the same stages of the tests for the TiN coatings of thicknesses 50 and 100 nm.

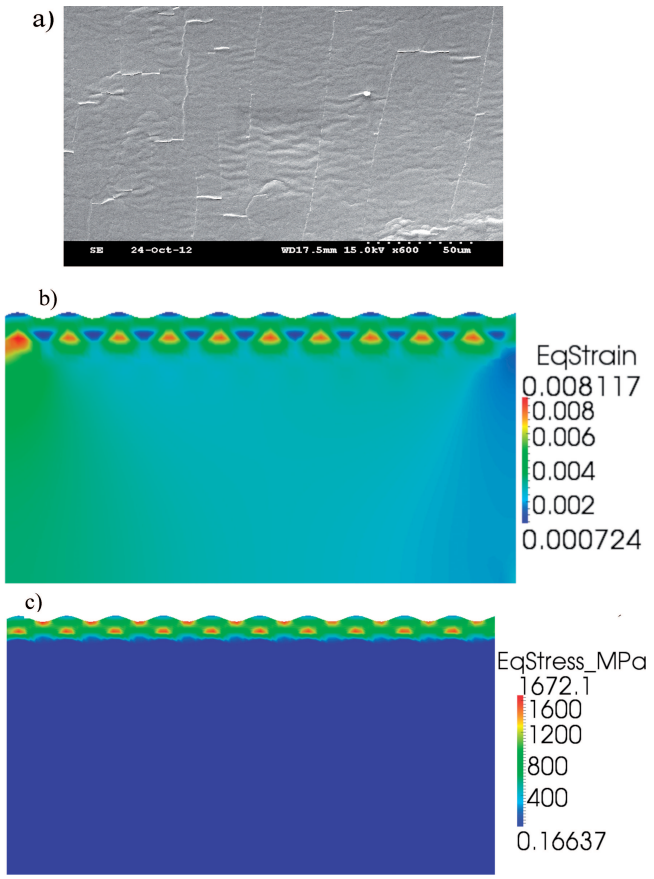

Fig. 9. The TiN coating of thickness 100 nm stretched at 15 N: a) SEM's image, b) effective strain in FE's micro model and c) mean stress in FE's micro model

TABLE 1

SEM's and FE's results

100 nm				50 nm			
force, N	SEM, mean X-strain (failure strain), ε_p	FE, effective strain, ε_i	FE, mean stress, MPa	force, N	SEM, mean X-strain, (failure strain), ε_p	FE, effective strain, ε_i	FE, mean stress, MPa
8	0.0011903	0.005202	1117.9	8	0.0011903	0.005474	1011.3
15	**0.0028368**	**0.008117**	**1672.1**	**15**	**0.0028368**	**0.008514**	**1509.4**
40	0.0109978	0.023063	2902.4	40	0.0109978	0.024203	2841.7

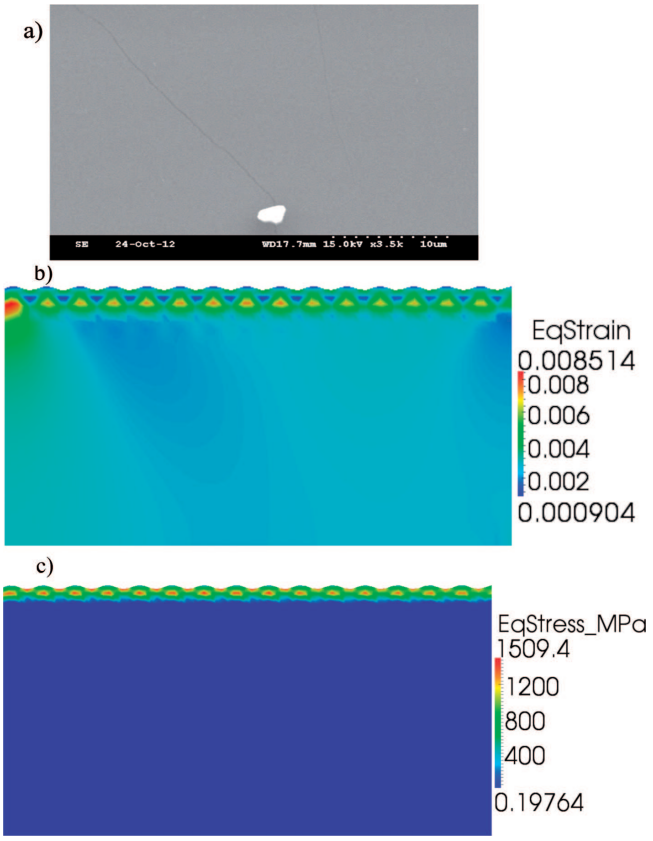

Fig. 10. The TiN coating of thickness of 50 nm stretched at 15 N: a) SEM's image, b) effective strain in FE's micro model and c) mean stress in FE's micro model

The cracking occurrence observed in experiments for failure strain (ε_p = 0.0028368) under middle loading conditions (15 N) corresponds to the FE' effective strain equal to ε_i = 0.008514 for the TiN coating of thickness 50 nm and to the FE's effective strain equal to ε_i = 0.008117 for the TiN coating of thickness 100 nm. Concluding, the set of fracture parameters (ductility function's parameters): ε_i and ε_p for the TiN coatings of thicknesses of 50 and 100 nm was identified.

4. Conclusion

Concluding, the FE micro model of multilayer wall of VAD enriched with fracture parameters developed in finite element code in the present work is able to predict the fracture probability. The micro model includes the surface's roughness and failure strain under tension condition for the TiN coatings of selected thicknesses. The developed micro model of wall of VAD can be applied in optimization procedures with respect to minimum of stress for the selected material system. The choice of the best construction of wall of LVAD have been realized by selection of material layers, substrates, thicknesses of material layers and selection of parameters of many deposition processes to obtain high quality coatings without fracture occurrence.

Acknowledgements

Financial assistance of the NCN, project no. 2011/01/D/ST8/04087, is acknowledged. The AFM's and SEM's studies were performed at the WIMiIP AGH. The polymer tension tests were performed at the Foundation of Cardiac Surgery Development in Zabrze, Poland.

REFERENCES

[1] Y. Mine, H. Fujisaki, M. Matsuda, M. Takeyama, K. Takashima, Microtension behaviour of TiAl polysynthetically twinned crystals with 0° – and 90° – oriented lamellae, Scripta Mater **65**, 707-710 (2011).

[2] S. Kumar, D.E. Wolfe, M.A. Haque, Dislocation shielding and flaw tolerance in titanium nitride, Int J Plasticity **27**, 739-747 (2011).

[3] J.L. Walley, R. Wheeler, M.D. Uchic, M.J. Mills, In-situ mechanical testing for characterizing strain localization during deformation at elevated temperatures, Exp Mech **52**, 405-416 (2012).

[4] L.M. Yin, X.P. Zhang, L. Chunsheng, Size and volume effects on the strength of microscale lead-free solder joints, J Electron Mater **38**, 2179-2183 (2009).

[5] Y.L. Su, S.H. Yao, C.S. Wei, C.T. Wu, W.H. Kao, Evaluation on the wear, tension and fatigue behavior of various PVD coated materials, Mater Lett **35**, 255-260 (1998).

[6] Y.L. Su, S.H. Yao, C.S. Wei, C.T. Wu, Tension and fatigue behavior of a PVD TiN-coated material, Thin Solid Films **315**, 153-158 (1998).

[7] P.A. Shade, R. Wheeler, Y.S. Choi, M.D. Uchic, D.M. Dimiduk, H.L. Fraser, A combined experimental and simulation study to examine lateral constraint effects on microcompression of single-slip oriented single crystals, Acta Mater **57**, 4580-4587 (2009).

[8] D. Kiener, P.J. Guruprasad, S.M. Keralavarma, G. Dehm, A.A. Benzerga, Work hardening in micropillar compression: In situ experiments and modeling, Acta Mater **59**, 3825-3840 (2011).

[9] Y. Gao, Z.L. Liu, X.C. You, Z. Zhuang, A hybrid multiscale computational framework of crystal plasticity at submicron scales, Comput Mater Sci **49**, 672-681 (2010).

[10] M. El Fray, A. Piegat, M. Czugała, Z. Staniszewski, M. Rybko, Nowe elastomerowe biomateriały dla systemów wspomagania pracy serca, in: R. Kustosz, M. Gonsior, A. Jarosz (Ed.), Technologie w inżynierii materiałowej i technologie metrologiczne dla potrzeb polskich protez serca, Epigraf Zabrze (2012).

[11] R. Kustosz, M. Gonsior, M. Gawlikowski, A. Jarosz, Biuletyn Programu Polskie Sztuczne Serce, Wydanie Specjalne – Rezultaty Programu, Epigraf Zabrze (2013).

[12] J. Kusiński, S. Kąc, Wytwarzanie techniką ablacji laserowej powłok na bazie Ti na podłożu polimerowym, in: R. Kustosz, M. Gonsior, A. Jarosz (Ed.), Technologie w inżynierii materiałowej i technologie metrologiczne dla potrzeb polskich protez serca, Epigraf Zabrze (2012).

[13] M. Kopernik, A. Milenin, Two-scale finite element model of multilayer blood chamber of POLVAD_EXT, Arch Civ Mech Eng **12**, 178-185 (2012).

[14] A. Milenin, M. Kopernik, Multiscale FEM model of artificial heart chamber composed of nanocoatings, Acta Bioeng Biomech **11**, 13-20 (2009).

[15] M. Kopernik, L. Trębacz, M. Pietrzyk, Modelling of fatigue behaviour of hard multilayer nanocoating system in nanoimpact test, in: V. Kompis (Ed.), Composites with micro- and nano-structures: computational modeling and experiments, Springer Liptovsky Mikulas (2008).

[16] S. Zhang, X. Zhang, Toughness evaluation of hard coatings and thin films, Thin Solid Films **520**, 2375-2389 (2012).

[17] A. Milenin, D.J. Byrska-Wójcik, O. Grydin, The multi-scale physical and numerical modelling of fracture phenomena in the MgCa0.8 alloy, Comput Struct **89**, 1038-1049 (2011).

[18] A. Milenin, M. Kopernik, D. Jurkojć, M. Gawlikowski, T. Rusin, M. Darłak, R. Kustosz, Numerical modelling and verification of Polish ventricular assist device, Acta Bioeng Biomech **14**, 49-57 (2012).

[19] U. Wiklund, J. Gunnars, S. Hogmark, Influence of residual stresses on fracture and delamination of thin hard coatings, Wear **232**, 262-269 (1999).

[20] A. Milenin, M. Kopernik, Microscale analysis of strain–stress state for TiN nanocoating of POLVAD and POLVAD_EXT, Acta Bioeng Biomech **13**, 11-19 (2011).

[21] M. Kopernik, Shape optimisation of a ventricular assist device using a VADFEM computer program, Acta Bioeng Biomech **15**, 81-87 (2013).

[22] M. Kopernik, A. Milenin, R. Major, J.M. Lackner, Identification of material model of TiN using numerical simulation of nanoindentation test, Mater Sci Tech **27**, 604-616 (2011).

[23] R. Major, E. Czarnowska, A. Sowińska, R. Kustosz, J. M. Lackner, W. Waldhauser, M. Woźniak, T. Wierzchoń, B. Major, e-Polymers **26**, 1-9 (2005).

[24] M. Kopernik, A. Milenin, S. Kąc, M. Wróbel, Stress-strain analysis in TiN nanocoating deposited on polymer with respect to Au nanointerlayer, J Nanometer, 1-12 (2014).

[25] J.M. Lackner, W. Waldhauser, P. Hartmann, O. Miskovics, F. Schmied, C. Teichert, T.Schöber, Self-assembling (nano-)wrinkling topography formation in low-temperature vacuum deposition on soft polymer surfaces, Thin Solid Films **520**, 2833-2840 (2012).

Received: 20 February 2014.